

Time-dependent deformation of polypropylene in response to different stress histories

B. E. Read and P. E. Tomlins*

Centre for Materials Measurement & Technology, National Physical Laboratory, Teddington, Middlesex, TW11 0LW, UK

(Received 22 May 1996; revised 21 November 1996)

Tensile strains have been determined as a function of time for polypropylene during (a) two-step loading, (b) creep recovery following removal of a load, and (c) intermittent load application. Data are presented at 23°C for specimens of different physical age, for different stress levels in the non-linear range and various durations of loading. The results are compared with predictions based on a pseudo-linear model. They have also been analysed using a modified superposition procedure that allows for changes in mean retardation time due both to physical ageing and to the application and removal of loads. This analysis has provided useful information on the variations of molecular mobility during the different loading histories. The functions and associated parameters used in the analyses could also form the basis of a method for presenting design data on plastics. Crown Copyright © 1997 Published by Elsevier Science Ltd.

(Keywords: physical ageing; creep; creep recovery)

INTRODUCTION

Boltzmann's Superposition Principle can be used to predict the deformation of polymeric solids subjected to arbitrary time-dependent loads¹. The success of this procedure requires that the viscoelastic behaviour is linear, implying that the applied stresses are sufficiently small to have a negligible effect on material properties. It also requires that no significant physical ageing and associated increase in retardation times occurs during the timescale of loading². Modifications to Boltzmann's Principle have been proposed to account for the effects of elevated stresses¹⁻⁵ and of physical ageing^{2,5}. However they have not provided accurate predictions of the strain-recovery following creep at high stress or of the non-linear response to more complex stress histories⁶.

In this article we describe studies of the non-linear, time-dependent strain in polypropylene at 23°C during (a) the two-step application of stresses, (b) creep recovery following removal of a stress and (c) the reapplication of a stress during creep recovery (intermittent loading). The experimental data have been analysed by a modified superposition procedure that allows for variations in mean retardation time due both to spontaneous physical ageing and to the application and removal of stresses. This approach represents an extension to our model for physical ageing and non-linear creep⁷⁻¹⁰, and is aimed at providing functions that could be employed in the design of plastic components subjected to time-varying loads.

SUMMARY OF CREEP MODEL

For a polymeric specimen subjected to a constant uniaxial tensile stress σ , the creep behaviour may be

specified by the compliance function, $D(t) = \epsilon(t)/\sigma$, where $\epsilon(t)$ is the time-dependent strain. Values of $D(t)$ are found to decrease with increasing physical age of the material, represented by the elapsed time t_e between cooling the specimen from a high temperature (at which the polymer structure is at equilibrium) and the start of the creep test². At stress levels below about 3 MPa, and for a given age t_e , $\epsilon(t)$ is usually proportional to σ for all times t and the linear creep behaviour may be characterized by a single $D(t)$ vs. $\log t$ curve. At higher stresses an increase of $D(t)$ with σ marks the onset of non-linear creep behaviour.

Various empirical functions have provided an accurate representation of the time-dependence of $D(t)$ for several glassy and semicrystalline plastics¹⁰. In previous investigations of polypropylene^{7,10}, and in the study reported here, we employed a stretched-exponential function of the form

$$D(t) = D_0 + \Delta D \left[1 - \exp \left(- \left(\int_0^t \frac{du}{\tau(u)} \right)^m \right) \right] \quad (1)$$

where D_0 is the compliance in the limit $t = 0$, ΔD is the retardation magnitude, $\tau(u)$ a mean retardation time for the creep process, and m a parameter ($0 < m \leq 1$) that characterizes the width of the retardation time distribution. The integral allows for changes in $\tau(u)$ due to physical ageing for all times (u) during the creep from 0 to t .

For several glassy and semicrystalline polymers, including polypropylene^{7,10}, a gradual decrease in D_0 with increasing age t_e has been successfully modelled. Within experimental error, no systematic variations of D_0 with σ are usually observed, and the value of m is essentially independent of t_e and σ ⁹.

* To whom correspondence should be addressed

The principal effect of increasing t_e (see Figure 1) is to shift the short-term region ($t < t_e$) of the $D(t) - \log t$ curve to longer times. This reflects an increase in the initial retardation time $\tau(0)$ at constant m . The decrease in slope of the compliance curve for $t > t_e$ (Figure 1) is then ascribed to an increase in $\tau(t)$ due to progressive ageing that accompanies the creep. This effect is allowed for by the integral in equation (1) assuming that D_0 and m are independent of creep time t .

With increasing stress (Figure 2), for a given age t_e , the short-term region of the compliance curve shifts to shorter times. This effect is opposite to that produced by physical ageing, and corresponds to a decrease in $\tau(0)$, although opinions differ as to whether it can be described as a stress-induced deageing of the material^{2,8,11,12}. The effects of progressive ageing during the creep are seen for stresses up to 9 MPa but at higher stresses they are obscured by an upturn in the creep curve at longer times, believed to mark the onset of a non-recoverable flow process¹³.

The theoretical fits shown to the creep curves in Figures 1 and 2 were obtained using equation (1), allowing for non-recoverable compliance contributions at 11.8 and 14.8 MPa, and the equation¹⁰

$$\tau(t) = (A^2 t_e^{2\mu} + C^2 t^{2\mu'})_{\sigma}^{0.5} \quad (2)$$

which describes the variation of τ for various polymers over wide ranges of t_e and t . The subscript σ is added to indicate that values for the parameters A , μ , C and μ' may each depend on stress level. These values usually decrease with increasing stress with $C \rightarrow A \rightarrow A_0$ and $\mu' \rightarrow \mu \rightarrow \mu_0$ in the limit $\sigma \rightarrow 0$. Table 1 lists values of the parameters derived from fitting equations (1) and (2) to the data in Figure 2, taking $\Delta D = 5.3 \text{ GPa}^{-1}$ and assuming that $\mu' = \mu$.

The variation of retardation time with t_e , stress and creep time is conveniently illustrated in Figure 3 by plots of $\log \tau(t)$ vs. $\log(t_e + t)$. The linear dependence of $\log \tau(0)$ on $\log t_e$ (exemplified by the results for $\sigma = 2.96 \text{ MPa}$) is consistent with the first term in brackets in equation (2), the values of μ and A corresponding to the respective slopes and intercepts (at $\log t_e = 0$) of such plots. Also shown is the abrupt decrease in τ and its subsequent increase with creep time (due to physical ageing) after applying various stresses at $t_e = 24 \text{ h}$. Values of μ' and C in equation (2) correspond to the slopes and intercepts, respectively, of the long-time asymptotes to these curves.

MODIFIED SUPERPOSITION ANALYSIS

Two-step load increase

It is convenient to consider first the response to a two-step loading in which a stress σ_0 is applied at $t = 0$ and an additional stress σ_1 at $t = t_1$ (see Figure 4a). For times $t \geq t_1$ the strain $\epsilon(t)$ is written as

$$\epsilon(t) = \epsilon_0(t) + \epsilon_1(t) \quad (3)$$

where $\epsilon_0(t)$ and $\epsilon_1(t)$ are the strain contributions due to stresses σ_0 and σ_1 , respectively, each of which operates indefinitely. On the basis of equations (1) and (3) we now write (assuming that D_0 , ΔD and m do not vary significantly with stress or with t and that $\mu = \mu'$)

$$\epsilon(t) = \sigma_0 \{ D_0 + \Delta D [1 - \exp(-(I_0 + I_1(t))^m)] \} + \sigma_1 \{ D_0 + \Delta D [1 - \exp(-I_1(t)^m)] \} \quad (4)$$

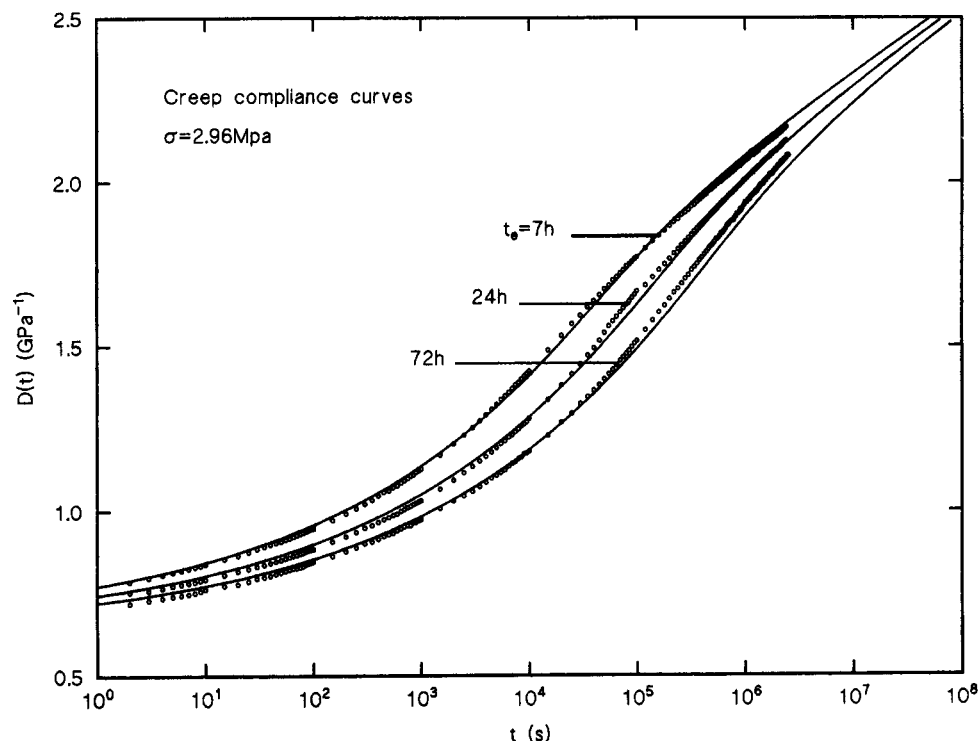


Figure 1 Tensile creep compliance curves for a stress of 2.96 MPa at different age stages t_e . Theoretical curves (—) were obtained by fitting equations (1) and (2) to the data

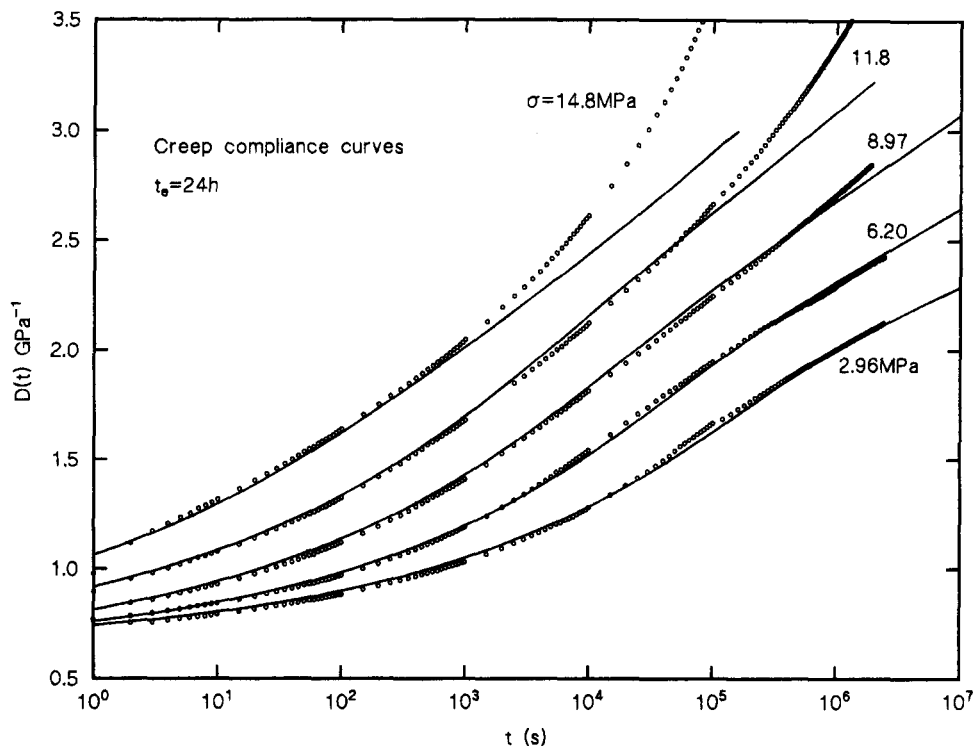


Figure 2 Tensile creep compliance curves for $t_e = 24$ h and different stress levels σ . The theoretical curves (—) were derived by fitting equations (1) and (2) to the data, taking $\Delta D = 5.3 \text{ GPa}^{-1}$ and yielding values for the other parameters given in Table 1

Table 1 Values of parameters obtained from modelling of creep curves

	Stress (MPa)				
	2.96	6.20	8.97	11.8	14.8
D_0 (GPa^{-1})	0.65	0.62	0.59	0.62	0.63
m	0.21	0.21	0.20	0.20	0.20
A ($s^{1-\mu}$)	56485	22890	14100	7560	2356
μ	0.71	0.63	0.54	0.47	0.40
C ($s^{1-\mu}$)	30000	30000	34000	28000	29900

where

$$I_0 = \int_0^{t_1} \frac{du}{(A^2 t_e^{2\mu} + C^2 u^{2\mu})^{0.5}} \quad (5)$$

and

$$I_1(t) = \int_{t_1}^t \frac{du}{\tau(u)} \quad (6)$$

The constant I_0 can be evaluated, using equation (5), from the parameters obtained by modelling the creep data during the first loading step. The integral $I_1(t)$ allows for changes in $\tau(t)$ for $t \geq t_1$ associated with spontaneous ageing and with the load increase at t_1 . It will be noted that $I_1(t)$ governs the behaviour of both $\epsilon_0(t)$ and $\epsilon_1(t)$ and can be determined (see Data analysis) using equation (4) from the measured $\epsilon(t)$ and the known value of I_0 . Instantaneous values of $\tau(t)$ can then be obtained from the relation

$$\frac{1}{\tau(t)} = \frac{dI_1(t)}{dt} = \frac{I_1(t) d \log I_1(t)}{t d \log t} \quad (7)$$

which follows from equation (6). Details will be given below of the procedures used to determine $\tau(t)$ (see Data

analysis) and of the function developed for describing its time-dependence, and hence the time-dependence of $\epsilon(t)$, during the second loading phase (see Two-step load increase).

Recovery following load removal

In this case (Figure 4b) a stress σ is applied at $t = 0$ and removed at $t = t_1$. The stress removal is equivalent to applying a negative stress of equal magnitude σ whilst preserving the original applied stress. We then have $\sigma_0 = \sigma$, $\sigma_1 = -\sigma$ and the strain components $\epsilon_0(t)$ and $\epsilon_1(t)$ are, respectively, positive and negative. Using equations (1) and (3) we now obtain for $t \geq t_1$

$$\epsilon(t) = \sigma \Delta D [\exp(-(I_1(t))^m) - \exp(-(I_0 + I_1(t))^m)] \quad (8)$$

where I_0 and $I_1(t)$ are given by equations (5) and (6) respectively.

Equation (8) may now be used to calculate values of $I_1(t)$ during the recovery phase from the known I_0 and measured $\epsilon(t)$, and the time-dependence of $\tau(t)$ subsequently evaluated using (7). A function used to model the variation of $\tau(t)$ during the recovery will be discussed in the section on Creep recovery.

Intermittent loading

As illustrated in Figure 4c, we now consider the response to a stress σ that is first applied at $t = 0$, removed at $t = t_1$, and subsequently reapplied at $t = t_2$. This loading history is equivalent to applying stresses $\sigma_0 = \sigma$, $\sigma_1 = -\sigma$ and $\sigma_2 = \sigma$ at times $t = 0$, t_1 and t_2 respectively. Superposition of the resulting strain components gives for $t \geq t_2$

$$\epsilon(t) = \epsilon_0(t) + \epsilon_1(t) + \epsilon_2(t) \quad (9)$$

where $\epsilon_0(t)$ and $\epsilon_2(t)$ have positive values and $\epsilon_1(t)$ is

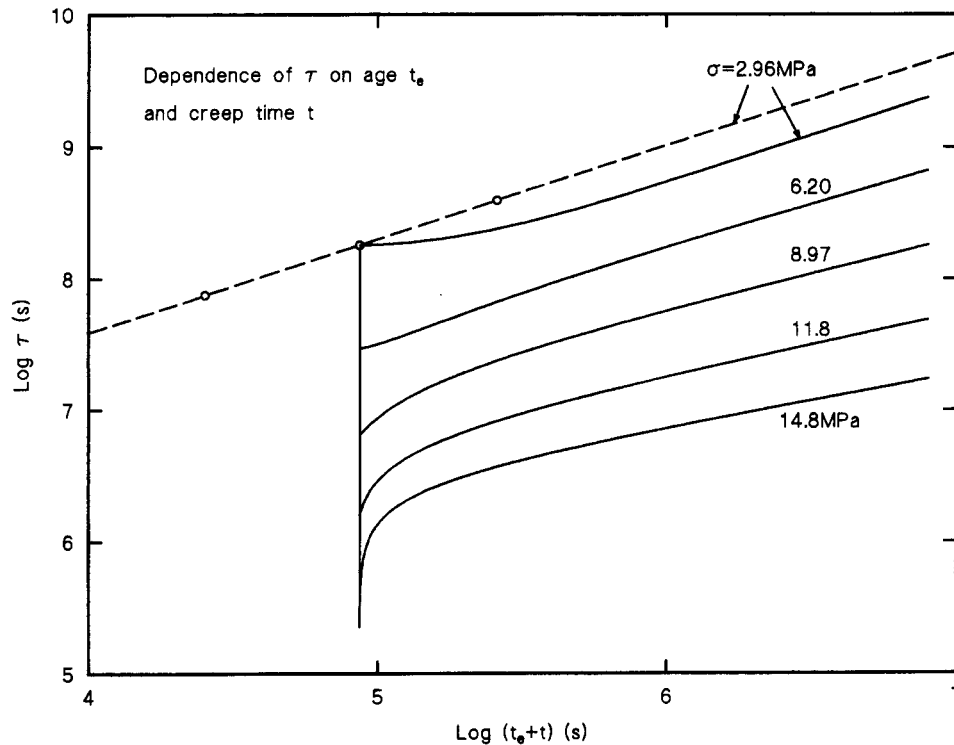


Figure 3 Double-logarithmic plots showing the variation of τ with age t_e and creep time t . (—○—), values of $\tau(0)$ at $t = 0$ for different t_e obtained from analyses of short-term creep data at 2.96 MPa. (—) Variations of $\tau(t)$ with t during long-term creep calculated from the data in Figure 2. These curves correspond to equation (2) with values of parameters from Table 1

negative. From equations (1) and (9) we have

$$\begin{aligned} \epsilon(t) = & \sigma \{ D_0 + \Delta D [1 - \exp(-(I_0 + I_1 + I_2(t))^m)] \} \\ & - \sigma \{ D_0 + \Delta D [1 - \exp(-(I_1 + I_2(t))^m)] \} \\ & + \sigma \{ D_0 + \Delta D [1 - \exp(-(I_2(t))^m)] \} \end{aligned} \quad (10)$$

where I_0 is given by equation (5) with $\sigma_0 = \sigma$,

$$I_1 = \int_{t_1}^{t_2} \frac{du}{\tau(u)} \quad (11)$$

and

$$I_2(t) = \int_{t_2}^t \frac{du}{\tau(u)} \quad (12)$$

The constant $I_1 [\equiv I_1(t_2)]$ may be evaluated using equation (8) from the known I_0 and the residual strain during the recovery at the instant of reloading. Values of $I_2(t)$ may then be obtained from equation (10) and the measured $\epsilon(t)$ for $t \geq t_2$. From equation (12) it follows that the corresponding $\tau(t)$ values during the second loading period can be estimated using

$$\frac{1}{\tau(t)} = \frac{dI_2(t)}{dt} = \frac{I_2(t)}{t} \frac{d \log I_2(t)}{d \log t} \quad (13)$$

The function used to model the time-dependence of $\tau(t)$ for $t \geq t_2$ will be considered in the section on Intermittent loading.

PSEUDO-LINEAR MODEL

For linear behaviour, and in the absence of ageing, the magnitude of each strain component will be proportional to the corresponding stress component at a given time after its application (and independent of other stress

components). In the case of a two-step load increase, this is represented by

$$\epsilon_1(t) = \frac{\sigma_1}{\sigma_0} \epsilon_0(t - t_1) \quad (14)$$

At elevated stresses, in the non-linear range, it will be instructive to compare the measured strains for $t \geq t_1$ with those predicted assuming the validity of equations (3) and (14). The predicted strains for $t \geq t_1$ are thus obtained using, in place of equation (4),

$$\begin{aligned} \epsilon(t) = & \sigma_0 \{ D_0 + \Delta D [1 - \exp(-(I'_0(t))^m)] \} \\ & + \sigma_1 \{ D_0 + \Delta D [1 - \exp(-(I'_1(t))^m)] \} \end{aligned} \quad (4a)$$

where

$$I'_0(t) = \int_0^t \frac{du}{(A^2 t_e^{2\mu} + C^2 u^{2\mu})_{\sigma_0}^{0.5}} \quad (15)$$

and

$$I'_1(t) = \int_{t_1}^t \frac{du}{(A^2 t_e^{2\mu} + C^2 (u - t_1)^{2\mu})_{\sigma_0}^{0.5}} \quad (16)$$

The values of A , μ and C in equations (15) and (16) are those obtained for stress σ_0 from fitting equations (1) and (2) to the creep data for $t \leq t_1$.

In the case of creep recovery, the pseudo-linear approximation assumes that

$$\epsilon_1(t) = -\epsilon_0(t - t_1) \quad (17)$$

and, from equation (3), the predicted strains for $t \geq t_1$ are obtained using

$$\epsilon(t) = \sigma \Delta D [\exp(-(I'_1(t))^m) - \exp(-(I'_0(t))^m)] \quad (8a)$$

where $I'_0(t)$ and $I'_1(t)$ are given by equations (15) and (16), respectively, with $\sigma_0 = \sigma$.

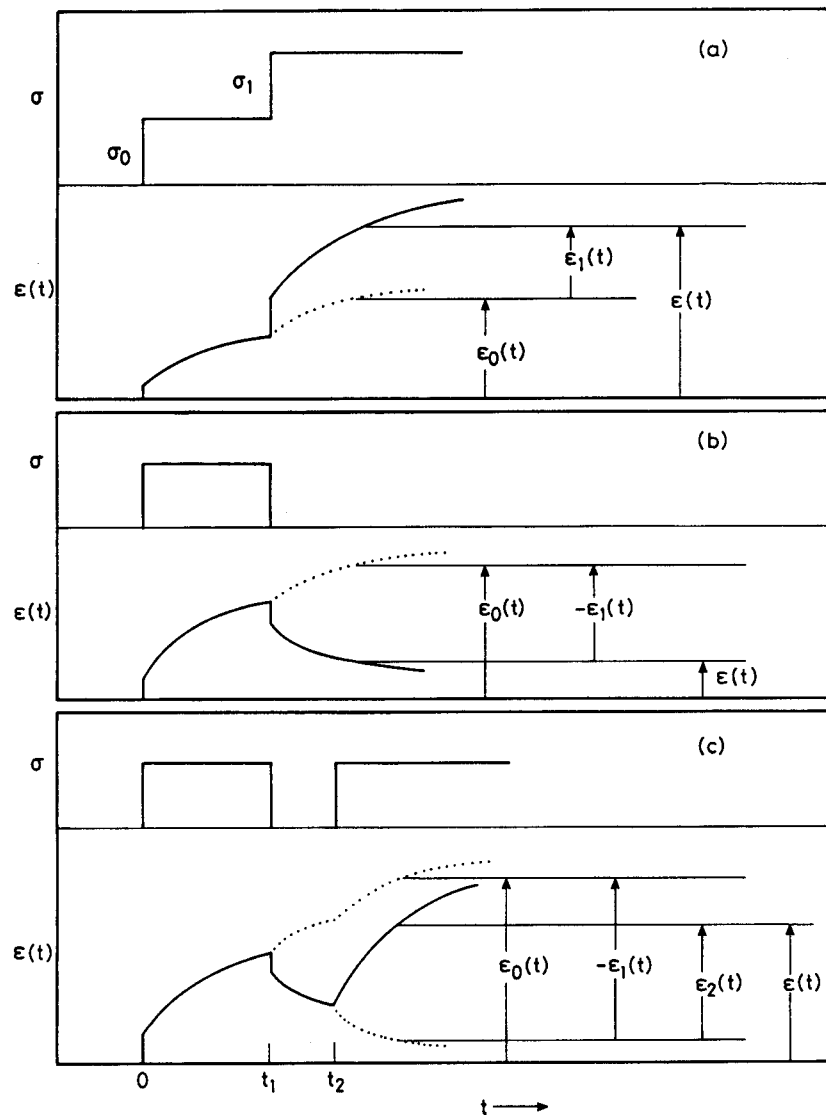


Figure 4 Schematic illustration of strain response to different stress histories. (a) Two-step load increase; (b) creep and subsequent recovery following load removal; (c) intermittent load application

For intermittent loading, the pseudo-linear scheme assumes the validity of equations (9) and (17) together with

$$\epsilon_2(t) = \epsilon_0(t - t_2) \quad (18)$$

The strains for $t \geq t_2$ are then predicted using the equation

$$\begin{aligned} \epsilon(t) = & \sigma \{ D_0 + \Delta D [1 - \exp(-(I'_0(t))^m)] \} \\ & - \sigma \{ D_0 + \Delta D [1 - \exp(-(I'_1(t))^m)] \} \\ & + \sigma \{ D_0 + \Delta D [1 - \exp(-(I'_2(t))^m)] \} \end{aligned} \quad (10a)$$

where $I'_0(t)$ and $I'_1(t)$ are again given by equations (15) and (16) with $\sigma_0 = \sigma$ and

$$I'_2(t) = \int_{t_2}^t \frac{du}{(A^2 t_e^{2\mu} + C^2 (u - t_2)^{2\mu})^{0.5}} \quad (19)$$

The pseudo-linear scheme cannot be generally valid since it implies that changes in $\tau(t)$ due to the application of σ_1 and σ_2 are negligible and makes no allowance for the effects of ageing during the periods $0 \rightarrow t_1$ and $0 \rightarrow t_2$ on the expressions for $I_1(t)$ and $I_2(t)$ respectively.

If the applied stresses are sufficiently small to have a negligible influence on $\tau(t)$ and, in addition, t is small compared with t_e so that changes in age state during the loading periods become negligible, then equations (15), (16) and (19) reduce to

$$I'_0(t) = \frac{t}{\tau(0)} \quad (20)$$

$$I'_1(t) = \frac{t - t_1}{\tau(0)} \quad (21)$$

$$I'_2(t) = \frac{t - t_2}{\tau(0)} \quad (22)$$

respectively, where $\tau(0) = At_e^\mu$. Substitution of these equations, into equations (4a), (8a) or (10a) yields the relations for linear viscoelasticity, usually derived without consideration for spontaneous ageing effects¹.

EXPERIMENTAL METHODS AND DATA ANALYSIS

Material

The polypropylene (Royalite, Propylex homopolymer)

was obtained in the form of a 9 mm thick sheet from VT Plastics (UK). Rectangular test pieces were machined from this sheet having nominal dimensions $180 \times 10 \times 4$ mm. To stabilize their crystallinity with respect to subsequent thermal treatments, the specimens were first annealed at 130°C for 4 h and then cooled slowly to room temperature. The density of the annealed material was determined by hydrostatic weighing in distilled water at 23°C and found to be 907 kg m^{-3} . This density corresponds to a calculated crystallinity of 61%¹⁴.

Prior to the initial load application, the specimens were heated to 80°C for 30 min to erase previous effects of ageing, quenched in water at 23°C , and stored at this temperature for different times t_e .

Strain and compliance determination

Tensile strains, $\epsilon_m(t) = \Delta l/l_0$, were determined from the measured time-dependent extensions Δl of specimens with unstrained gauge length l_0 . Each specimen was held vertically between a fixed lower clamp and an upper clamp through which loads were applied via a pivoted lever arm with a 5/1 ratio advantage. Two calibrated extensometers of gauge length 50 mm were located on opposite faces of the specimen. The extensometers each comprised an inductive displacement transducer that contacted the specimen via two knife edges¹⁵. One of the knife edges was attached to the core of the transducer and the other to its body. A data logger was employed to sample the amplified output voltage from each extensometer at specified time intervals. The first recordings were made at 1 s after the application or removal of a load. At the end of each loading or unloading period, the data were dumped to a disc for storage and subsequent analysis. All measurements were made at $23.0 \pm 0.2^\circ\text{C}$ by locating the specimens in temperature-controlled chambers.

Corrections to the measured strains $\epsilon_m(t)$ were made to account for the small variations in cross-sectional area, and hence true stress, that accompany the length changes at constant load. The corrected strains $\epsilon(t)$ and derived compliances $D(t)$ are related by

$$\epsilon(t) = \epsilon_m(t)[1 - 2\nu\epsilon_m(t)] = D(t)\sigma_u \quad (23)$$

where σ_u is the calculated stress per unit unstrained cross-sectional area and a value of 0.37 was taken for Poisson's ratio ν . For a specimen of given age, the strains and compliances were usually reproducible to within 2%.

Data analysis

Values of the parameters D_0 , m , A , μ and C are required to calculate the strains for any loading sequence according to the modified superposition procedure or pseudo-linear model. Taking $\Delta D = 5.3 \text{ GPa}^{-1}$, D_0 , m and $\tau(0)$ were first obtained by fitting equation (1) to the initial parts of the creep curves¹⁶ spanning the time range $t \leq 0.2t_e$. Noting that the effective age of a testpiece does not change significantly over this period, the integral of equation (1) then becomes $t/\tau(0)$ where $\tau(0) = At_e^\mu$. A and μ were subsequently derived from the respective intercept and slope of a plot of $\log \tau(0)$ vs. $\log t_e$. For creep times in excess of the short-term limit ($0.2t_e$) the effective age of the testpiece progressively increases and the data have to be modelled in terms of equation (1)

with $\tau(u)$ given by equation (2). The only unknown variable in these equations, C , was obtained by a linear least-squares fit to the data¹⁷ noting that the integral of equation (1) has to be solved numerically.

Within experimental error, D_0 and m showed no systematic variations with stress whereas A , μ and C were found to be stress dependent although independent of elapsed time, t_e . By using the optimum values of these parameters for each of the loading sequences, allowance was made for the lack of exact repeatability of experimental results.

Values for the unknown integral $I_1(t)$ in equations (4) and (8) were obtained by a linear least-squares fit of these functions to experimental data using appropriate values of D_0 , m , A , μ and C . The time dependence of the mean retardation time $\tau(t)$ was obtained by differentiating a polynomial fit¹⁸ to the plot of $\log I_1(t)$ vs. $\log t$ following equation (7). Similar procedures were employed to determine $I_2(t)$ in equation (10) and the corresponding $\tau(t)$ according to equation (13). The modelling of $\tau(t)$ is discussed in the following section.

RESULTS AND DISCUSSION

Two-step load increase

Figure 5 shows the measured strains as a function of $\log t$ in a two-step loading test on a specimen of age $t_e = 24$ h. The specimen was first subjected to a stress $\sigma_0 = 6.2 \text{ MPa}$ at $t = 0$ and an additional stress of $\sigma_1 = 5.7 \text{ MPa}$ was then applied at $t_1 = 6$ h. For comparison, creep strains are also presented for another specimen of age $t_e = 24$ h subjected to a stress of 11.9 MPa at $t = 0$. For times greater than about 30 h, the effects of the second loading step become dominant and the strains produced by the different stress histories are seen to converge.

During the second loading stage, the observed strains are much larger than those predicted by the pseudo-linear scheme (Figure 5). This result is ascribed to a decrease in τ due to the second load increase, an effect which serves to increase both $\epsilon_0(t)$ and $\epsilon_1(t)$ but is not accounted for by the pseudo-linear approximation.

Figure 6 shows a plot of $\log \tau(t)$ vs. $\log(t_e + t)$ calculated from the strain data of Figure 5 according to the modified superposition procedure [equation (7)]. The application of σ_1 is seen to produce an abrupt decrease in $\tau(t)$ to values somewhat lower than those calculated from the creep data at 11.9 MPa . Subsequently the $\tau(t)$ values increase, due to a reactivation of ageing, to a level close to that derived for 11.9 MPa . The retardation time thus appears to depend on the effective age of the material and the total instantaneous applied stress. It is also found that the increase in $\tau(t)$ after the second load application can be described to a good approximation by the power law

$$\log \tau(t) = \log \tau_1 + k_1(t - t_1)^{m_1} \quad (24)$$

where τ_1 is the mean retardation time at t_1 immediately following the application of σ_1 , and k_1 and m_1 are constants. Table 2 lists the values of the parameters obtained from the data in Figure 6 and from similar results for different t_1 and σ_1 . On the basis of equation (24), the time-dependence of $\epsilon(t)$ for $t \geq t_1$ has been

modelled using equations (4), (5) and (6) with

$$\tau(u) = 10^{(\log \tau_1 + k_1(u-t_1)^{m_1})} \quad (25)$$

Figure 5 illustrates the good agreement between the calculated and measured strains.

Creep recovery

The recovery data will be illustrated by plots of the residual strain vs. $\log(t - t_1)$ rather than $\log t$. By effectively expanding the timescale at short recovery times, this allows the proposed recovery functions to be more accurately assessed in this region.

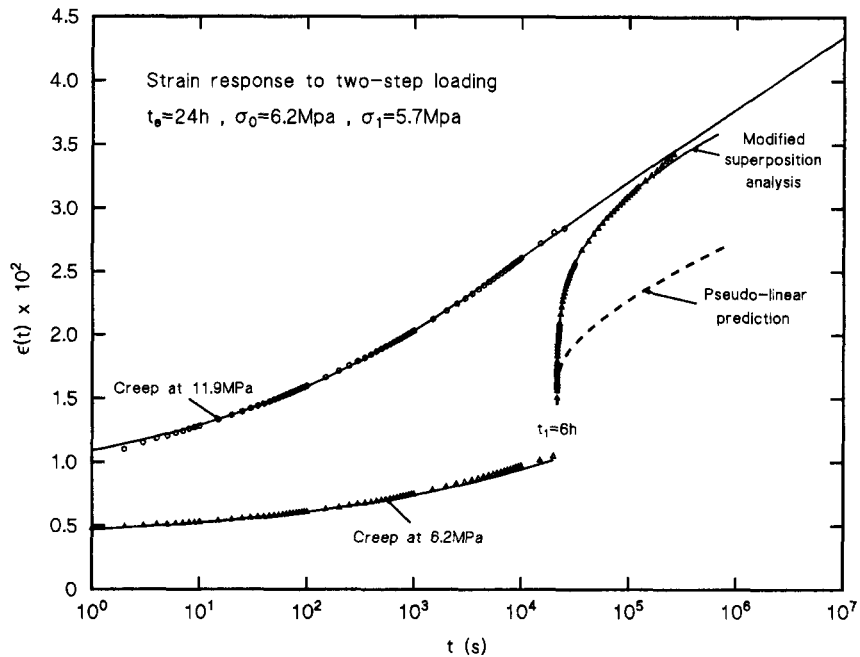


Figure 5 (Δ) Time-dependence of the strain during a two-step loading test with $t_e = 24$ h, $\sigma_0 = 6.2$ MPa, $\sigma_1 = 5.7$ MPa and $t_1 = 6$ h. (○) Strains determined during a single-creep test for $t_e = 24$ h and $\sigma = 11.9$ MPa. (---) Predicted strains during the second loading stage according to equation (4a), with parameters for 6.2 MPa from Table 1. (—) Calculated strains obtained by fitting equations (1) and (2) to data in the first loading stage and using equations (4) and (25) in the second stage. Using equations (1) and (2), the parameters obtained for 6.2 MPa are given in Table 1 and, for 11.9 MPa, we obtained $m = 0.20$, $D_0 = 0.62 \text{ GPa}^{-1}$, $A = 6837 \text{ s}^{1-\mu}$, $C = 20000 \text{ s}^{1-\mu}$ and $\mu = \mu' = 0.47$. Using equations (4) and (5), values of the parameters were taken from Table 1 for 6.2 MPa. The parameters used with equation (25) are listed in Table 2

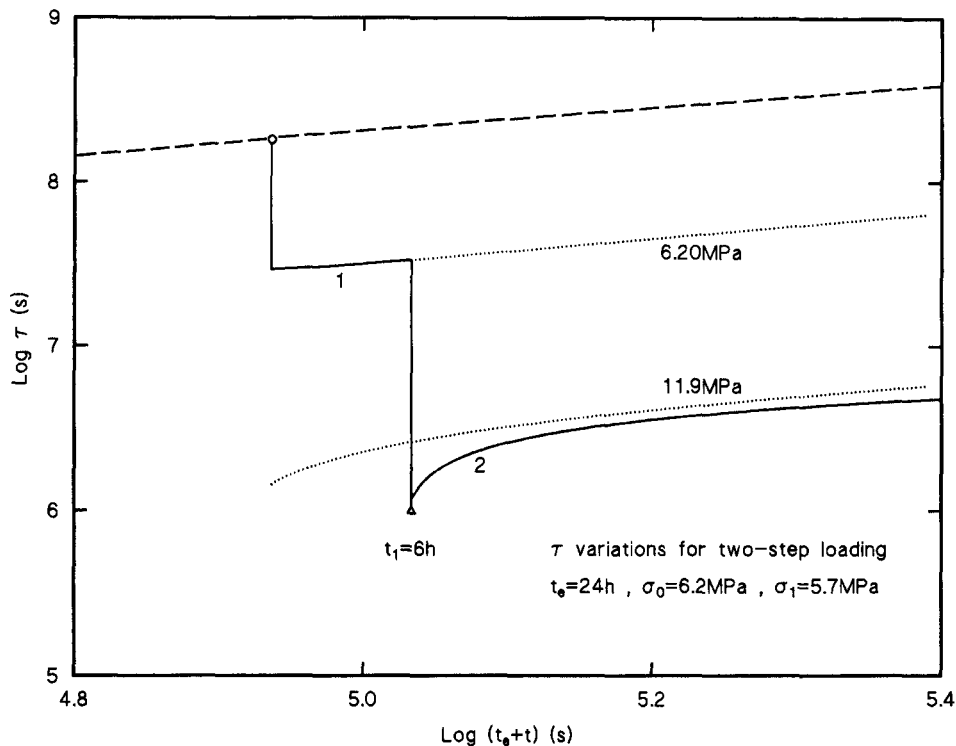


Figure 6 (—) Calculated variation of $\tau(t)$ with t from the experimental data in Figure 5 during the first stage (1) and second stage (2) of the two-step loading test. In stage 1, $\tau(t)$ values are given by equation (2) with parameters from Table 1. In stage 2, $\tau(t)$ calculated from the modified superposition equations as described in the text. (—○—). As in Figure 3. (···) Variation of $\tau(t)$ during long-term creep at the specified stresses according to equation (2) with parameters from Table 1 and Figure 5. (Δ) τ_1 value at $t = t_1$ from Table 2

Table 2 Values of parameters describing the variation of $\tau(t)$ during the second stage of two-step loading tests ($t_e = 24$ h)

σ_0 (MPa)	σ_1 (MPa)	t_1 (s)	$\log \tau_1$ (s)	k_1 (s^{-m_1})	m_1
6.2	5.70	3633	5.85	0.061	0.231
6.2	5.70	21 600	5.99	0.022	0.302
6.2	2.85	3774	6.70	0.014	0.316

Pseudo-linear model. Figures 7 and 8 show creep and recovery curves at a stress close to 3 MPa that is just within the non-linear range. When the duration of the test is short compared with t_e (Figure 7) the pseudo-linear scheme provides a good description of the behaviour. This is consistent with the fact that equation (15) then reduces to equation (20) and, similarly, equation (16) reduces to equation (21). Hence the behaviour conforms

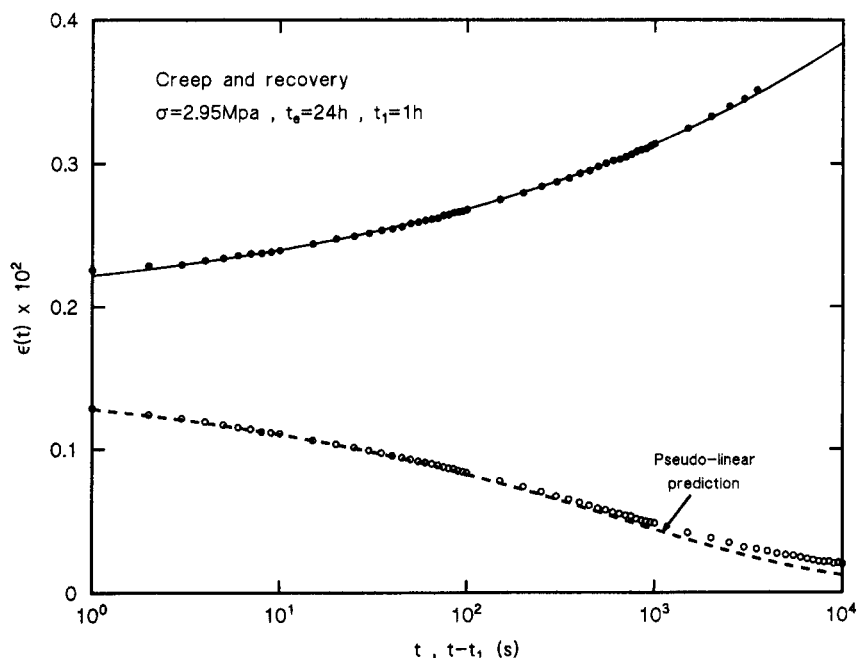


Figure 7 Low-stress creep (●) and recovery (○) data for $t_e = 24$ h, $\sigma = 2.95$ MPa and $t_1 = 3687$ s. (—) Fit of equations (1) and (2) to the creep data. (- - -) Predicted recovery using equation (8a). Values for parameters as follows: $D_0 = 0.65 \text{ GPa}^{-1}$, $\Delta D = 5.3 \text{ GPa}^{-1}$, $m = 0.21$, $A = 50 100 \text{ s}^{1-\mu}$, $C = 30 000 \text{ s}^{1-\mu}$, $\mu = \mu' = 0.71$

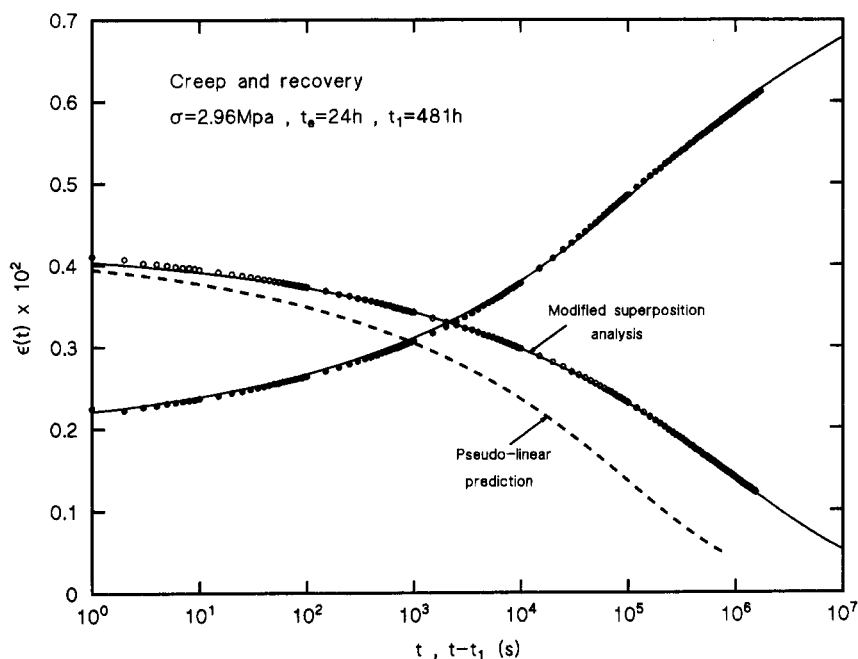


Figure 8 Low-stress creep (●) and recovery (○) data for $t_e = 24$ h, $\sigma = 2.96$ MPa and $t_1 = 481$ h. (—) Fit of equations (1) and (2) to the creep data and calculated recovery curve using equations (8) and (26) with values of parameters in Tables 1 and 3. (- - -) Predicted recovery using equation (8a) with values of parameters given in Table 1

closely with the equations of linear viscoelasticity. However for creep times t_1 much larger than t_e then, as shown in Figure 8, the observed strains during the recovery are substantially larger than those predicted by the pseudo-linear approximation. The discrepancy is attributed to physical ageing that occurs during the creep, as a result of which $\tau(t)$ values during the recovery are higher than those in the early stages of the creep. Thus the magnitude of the negative $\epsilon_1(t)$ component is smaller than that predicted by equation (17).

At elevated stresses (see Figure 9) the measured strains at long recovery times are again larger than those predicted by the pseudo-linear model. However at short recovery times (for t_1 small compared with t_e) they are significantly smaller than the predicted values (see also Figure 12 below), suggesting a possible decrease in τ on unloading and consequent increase in the relative magnitude of $\epsilon_1(t)$.

Modified superposition analysis. With the aid of methods detailed in Data analysis, equations (7) and (8) were employed to derive $\tau(t)$ from the measured strains during creep recovery for several combinations of σ , t_e and t_1 . Some results of these calculations are included in Figure 10 for the case $\sigma = 11.8$ MPa, $t_1 = 1$ h and different age states t_e . Figure 11 shows similar data for a stress of 8.97 MPa, $t_e = 24$ h and various creep durations t_1 . It will be observed that the retardation time exhibits an abrupt decrease upon load removal, and then increases quite rapidly to a level close to that found for $\sigma \rightarrow 0$ from low-stress creep data. In support of the latter observation, Figure 11 shows that retardation times determined from low-stress creep measurements after reloading the specimens during recovery lie close to the extrapolated values from low-stress data prior to the application of an elevated stress. The small discrepancies between the calculated $\tau(t)$ from the recovery data and the retardation times for the reloaded

specimens could reflect inaccuracies in the form of the creep function over wide time ranges.

The increase of $\tau(t)$ over 4–5 decades of recovery time can be closely described by the power-law function

$$\log \tau(t) = \log \tau_{1r} + k_r(t - t_1)^{m_r} \quad (26)$$

where τ_{1r} is the initial retardation time governing the recovery at the instant of unloading ($t = t_1$) and k_r and m_r are constants. The derived values for τ_{1r} , k_r and m_r are shown in Table 3 and were used to recalculate the residual strains using equations (8), (5), (6) and (26). Figures 8 and 9 exemplify the excellent agreement typically observed between the experimental and calculated strains.

Further work is required to develop functions that relate τ_{1r} , k_r and m_r to the variables σ , t_e and t_1 and that may serve as a basis for predicting the recovery behaviour. Some comments can, however, be made on the significance of, and possible method for estimating, these parameters.

Regarding the value of $\log \tau_{1r}$, this will depend on the retardation time τ_{1c} during the creep at $t = t_1$ and the decrease $\Delta \log \tau_1 = \log \tau_{1c} - \log \tau_{1r}$ due to unloading. According to our model, this decrease is produced by the negative (compressive) component of the deconvoluted stress and could reflect a transient structural change in the material (increase in free volume or conformational entropy). From studies of PVC, we have found that the retardation time for short-term creep under uniaxial compression decreases with increasing stress, the magnitude of this decrease being around 40% of that observed under tension⁹. From the data in Tables 1 and 3 we estimate that the magnitude of $\Delta \log \tau_1$ is about 60% of the decrease in $\log \tau$ produced by the initial loading, or about 40% of the decrease produced by an additional load of the same magnitude. Based on these observations, it appears that close estimates of $\log \tau_{1r}$ could be obtained from a combined analysis of tensile and compressive creep data.

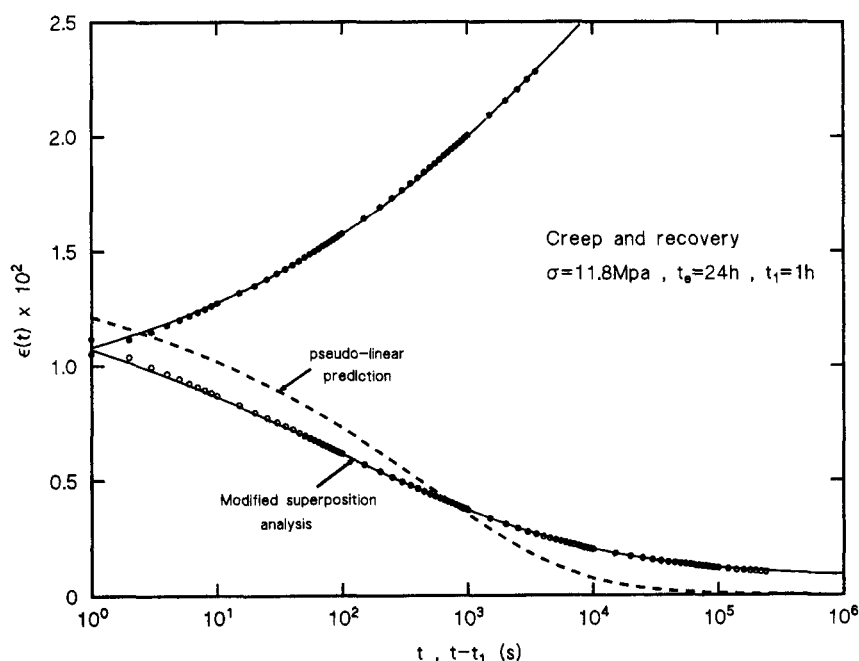


Figure 9 Creep (●) and recovery (○) data for $t_e = 24$ h, $\sigma = 11.8$ MPa and $t_1 = 3600$ s. Theoretical curves (—) and (---) derived as in Figure 8

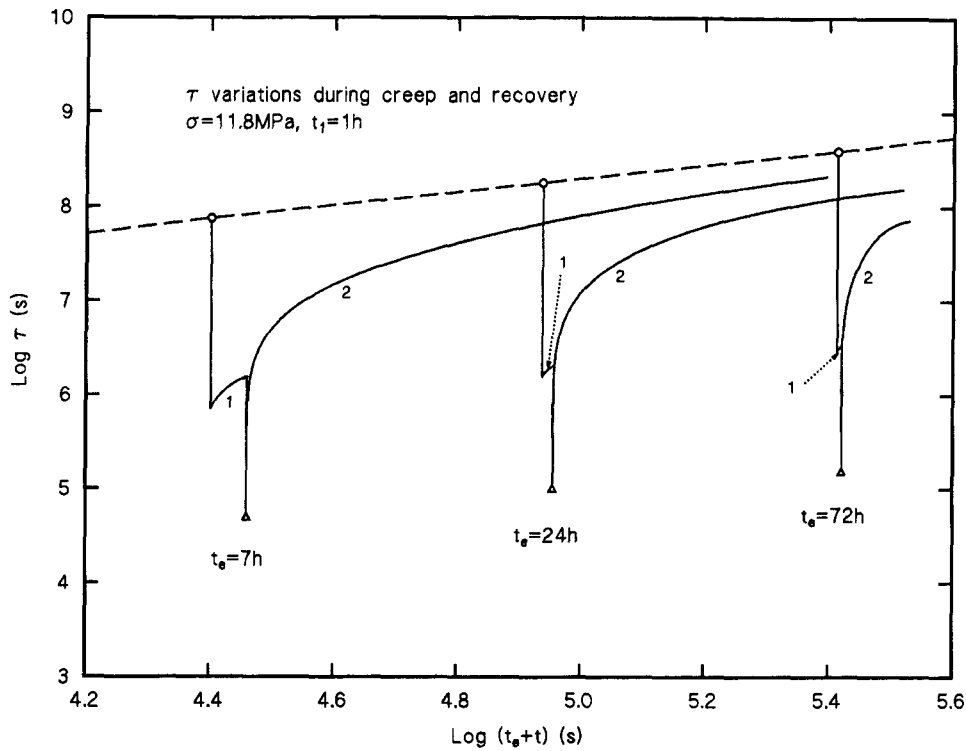


Figure 10 (—) Calculated variation of $\tau(t)$ with t during the creep (1) and recovery (2) for $\sigma = 11.8$ MPa, $t_1 \approx 1$ h and different t_e . $\tau(t)$ values during creep are given by equation (2) with parameters in Table 1. During the recovery, $\tau(t)$ calculated by the modified superposition procedure described in the text. (—○—) As in Figure 3. (Δ) τ_{1r} values at $t = t_1$ from Table 3

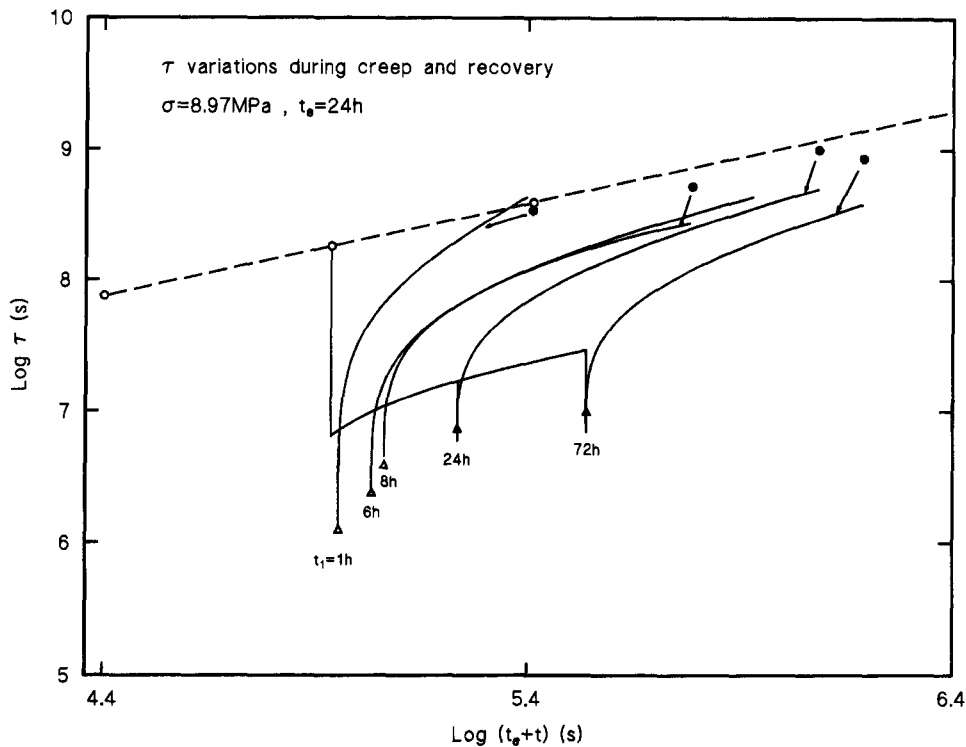


Figure 11 (—) Variations of $\tau(t)$ with t during creep and recovery for $\sigma = 8.97$ MPa, $t_e = 24$ h and different creep durations t_1 . Calculations and symbols (—○—), (Δ) as in Figure 10. (●) τ values determined during recovery from short-term creep data after reapplying a stress of 2.96 MPa

With regard to the value of k_r and m_r , we note that equation (26) could reflect a progressive decrease in free volume or conformational entropy during the recovery since $\log \tau(t)$ should be inversely proportional to each of these structural variables¹. The parameter k_r will then

characterize the rate of the structural recovery and depend on the magnitude and some time constant for the structural process. It will be evident from Table 3 that trends in the value of k_r with varying σ , t_e and t_1 , respectively, are opposite to the trends in $\log \tau_{1r}$. This

suggests that related empirical relationships could be developed for modelling variations in τ_{1r} , k_r and m_r .

Intermittent loading

Figure 12 presents the measured strains produced by intermittent loading for $\sigma = 9.02$ MPa, $t_e = 24$ h, $t_1 = 1.09$ h and $t_2 = 2.09$ h. During the recovery stage ($t_2 \geq t \geq t_1$), the discrepancies between the observed strains and those predicted by the pseudo-linear scheme are again indicative of an abrupt decrease and

Table 3 Values of parameters describing the variation of $\tau(t)$ during creep recovery

Stress (MPa)	t_e (h)	t_1 (s)	$\log \tau_{1r}$ (s)	k_r (s^{-m_r})	m_r
2.96	24	1.731×10^6	8.917	0.088	0.105
6.20	24	3760	6.964	0.104	0.224
	24	21330	7.142	0.050	0.259
8.97	7	3700	5.502	0.362	0.167
	24	1822	5.778	0.271	0.198
	24	3600	6.091	0.203	0.211
	24	21393	6.374	0.106	0.235
	24	28800	6.582	0.076	0.253
	24	85181	6.862	0.028	0.313
	24	260246	6.989	0.024	0.303
	72	3650	5.945	0.329	0.164
11.8	7	3600	4.687	0.641	0.145
	24	1800	4.921	0.604	0.148
	24	3600	4.992	0.514	0.153
	24	28800	5.240	0.393	0.160
	72	3900	5.177	0.477	0.157
14.8	7	2160	3.154	1.450	0.102
	24	2045	3.307	1.389	0.110
	72	2160	3.567	1.293	0.104

subsequent increase in $\tau(t)$ following the load removal at t_1 . The retardation times calculated with the aid of equation (7) are included in Figure 13, and it is seen (Figure 12) that the residual strains during the recovery can again be accurately modelled by the modified superposition equations.

The initial strain increment due to the reloading at t_2 is somewhat larger than that predicted by the pseudo linear scheme (Figure 12). This is consistent with the observation in Figure 13 that the reloading occurs before $\tau(t)$ has increased to the zero-stress level and produces a further sharp decrease in $\tau(t)$ to a value below that observed after the first loading. For $t > t_2$, $\tau(t)$ then increases quite rapidly to the level calculated for continuous loading. The latter increase can be described to a good approximation by the function

$$\log \tau(t) = \log \tau_2 + k_2(t - t_2)^{m_2} \quad (27)$$

where τ_2 is the mean retardation time at t_2 immediately after the reloading and k_2 and m_2 are constants. Figure 12 shows the good agreement between the observed strains for $t \geq t_2$ and those calculated by the modified superposition analysis with the aid of equations (26) and (27).

Similar results have been obtained from intermittent loading tests in which the recovery period ($t_2 - t_1 \approx 1$ h) is short compared with the initial creep duration ($t_1 = 6$ h and 24 h respectively). When the recovery period is long compared with the creep duration it is expected that $\tau(t)$ will increase to around the zero-stress level prior to the reloading. Owing to the increase in effective age of the material between $t = 0$ and $t = t_2$, the $\tau(t)$ value after reloading should then be higher than that observed after the initial loading. This would explain previous observations⁶ that the strain increment produced by reloading

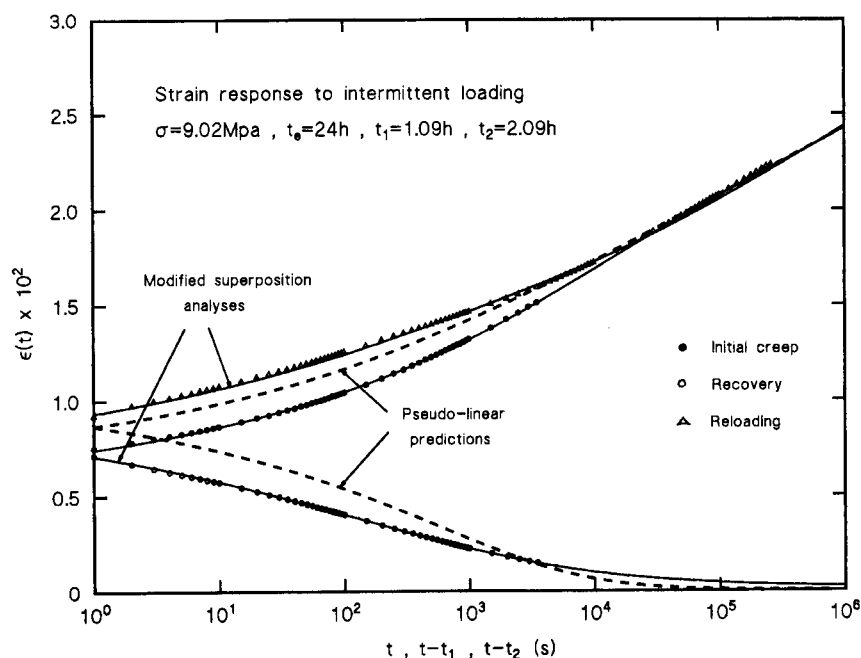


Figure 12 Time-dependence of the strain during the initial creep (●) and recovery (○), and after reloading (△), for an intermittent load test with $\sigma = 9.02$ MPa, $t_e = 24$ h, $t_1 = 3910$ s and $t_2 = 7515$ s. (---) Pseudo-linear predictions using equation (8a) for recovery and (10a) after reloading. (—) Calculated strains using equations (1) and (2) for the initial creep, equation (8) for the recovery and equation (10) after reloading. Parameters as follows: $D_0 = 0.62$ GPa⁻¹, $m = 0.20$, $A = 11517$ s^{1- μ} , $\mu = 0.54$, $C = 34000$ s^{1- μ} . Values of $\tau(u)$ in equations (6) and (11) calculated using equation (26) with $\log \tau_{1r} = 5.621$, $k_r = 0.410$ s^{- m_r} , $m_r = 0.146$. Values of $\tau(u)$ in equation (12) calculated using equation (27) with $\log \tau_2 = 6.00$, $k_2 = 0.312$ s^{- m_2} , $m_2 = 0.123$

duration of loading.

ACKNOWLEDGEMENTS

The research described in this report was funded by the UK Department of Trade and Industry as part of their programme on Measurement, Technology and Standards for Advanced Materials.

Durham, North Carolina, USA. Financed and Distributed by Biosoft, Cambridge UK and Ferguson, MO, USA.

17. Mathcad V. 5.0 Plus, Mathsoft Inc., Cambridge, Ma, USA.
18. Plots of $\log I_1(t)$ vs. $\log t$ were initially described by Chebyshev polynomials which were subsequently differentiated to give $\tau(t)$. Fitting and differentiation of these plots was carried out using Matlab (Version 4.1, Mathworks Inc., USA) together with software from the National Physical Laboratories Data Approximation Subroutine Library.